Original Article

Hippocampal amide proton transfer values are associated with cerebral small vessel disease imaging markers and total burden: a community-based cross-sectional study

Ronghua Mu[1#], Xiaoyan Qin[1#], Wei Zheng[1#], Peng Yang[1], Bingqin Huang[1,2], Xin Li[1], Fuzhen Liu[1], Kan Deng[3], Xiqi Zhu[4]

[1]Department of Radiology, Nanxishan Hospital of Guangxi Zhuang Autonomous Region, Guilin, China; [2]Graduate School, Guilin Medical University, Guilin, China; [3]Philips (China) Investment Co., Ltd., Guangzhou Branch, Guangzhou, China; [4]Department of Radiology, The Affiliated Hospital of Youjiang Medical University for Nationalities, Baise, China

Contributions: (I) Conception and design: R Mu, X Qin, W Zheng, X Zhu; (II) Administrative support: R Mu, X Qin, W Zheng, X Zhu; (III) Provision of study materials or patients: R Mu, X Qin, W Zheng, X Zhu; (IV) Collection and assembly of data: All authors; (V) Data analysis and interpretation: R Mu, X Qin, W Zheng, B Huang, X Zhu; (VI) Manuscript writing: All authors; (VII) Final approval of manuscript: All authors.

[#]These authors contributed equally to this work.

Correspondence to: Xiqi Zhu, MD, PhD. Department of Radiology, The Affiliated Hospital of Youjiang Medical University for Nationalities, No. 18 Zhongshan Second Road, Baise 533000, China. Email: xiqi.zhu@163.com.

Background: Neurodegeneration has been suggested to be associated with cerebral small vessel disease (CSVD). The association between different CSVD imaging markers and the extent of neurodegeneration could be indirectly confirmed by examining the relationship between CSVD imaging markers and the hippocampal amide proton transfer (APT) values. The associations between hippocampal APT values with CSVD imaging markers and CSVD total load need to be further validated. The aim of this study was to investigate potential variations in hippocampal APT values among individuals with CSVD imaging markers and varying degrees of CSVD total burden.

Methods: A cross-sectional study (retrospective analysis of prospectively-acquired data) was conducted at Nanxishan Hospital of Guangxi Zhuang Autonomous Region. From May 2020 to June 2021, 165 individuals (age, 40–76 years; male/female, 103/62) were included in this study. The inclusion criteria for the participants were as follows: The presence of lacunar infarction (LI), and/or cerebral microbleed (CMB); moderate-to-severe enlarged perivascular space (EPVS) (>20); deep white matter hyperintensity (WMH) > Fazekas 2 or periventricular WMH > Fazekas. The exclusion criteria comprised the following: History of craniocerebral operation; Cases with significant pathology incidentally identified during magnetic resonance (MR) scan; Drug or alcohol abuse. The differences of hippocampal APT values between CSVD imaging makers presence or absence groups and different CSVD total burden groups were compared using independent *t*-test and one-way analysis of variance (ANOVA). The correlations between APT values and CSVD imaging markers were analyzed using Pearson correlation analysis. A mediation analysis model was used to investigate the mediating effect of the hippocampal APT values in the association between CSVD total loads and Montreal Cognitive Assessment (MoCA) score was assessed.

Results: The hippocampal APT values among different CSVD total load groups were significantly different (P<0.001). The hippocampal APT values were significantly different between the imaging markers presence and absence groups. The P values for the LI, WMH EPVS, and CMB presence or absence groups were <0.001, <0.001, 0.034, and 0.002, respectively. The hippocampal APT values were significantly correlated with CMB (P<0.01), LI (P<0.01) and WMH (P<0.01). The mediation models demonstrated that

the APT values of the hippocampus partially mediated the association between CSVD total load and MoCA score, the proportion of mediation attributable was calculated as 17.50%.

Conclusions: Hippocampal APT values were associated with CSVD imaging markers and total burden. Hippocampal APT values may serve as a biomarker for the early detection of neurodegeneration in CSVD patients.

Keywords: Cerebral small vessel disease (CSVD); neurodegenerative disease; amide proton transfer (APT); Montreal Cognitive Assessment (MoCA); hippocampus

Submitted Oct 20, 2023. Accepted for publication Jan 23, 2024. Published online Mar 04, 2024.
doi: 10.21037/qims-23-1464
View this article at: https://dx.doi.org/10.21037/qims-23-1464

Introduction

Cerebral small vessel disease (CSVD) has been considered a disorder that primarily affects cerebral microvessels, making it the most prevalent form of vascular cognitive impairment and a significant contributor to mixed dementia (1,2). Magnetic resonance imaging (MRI) displays diverse characteristics of CSVD, including ischemic lesions such as white matter hyperintensities (WMH) and lacunar infarctions (LI), as well as hemorrhagic lesions known as cerebral microbleeds (CMB) (3,4). Other neuroimaging changes include recent small subcortical infarction and enlarged perivascular space (EPVS) (3). Brain atrophy has also been linked to CSVD (5). However, none of these CSVD imaging markers provide insights into the pathophysiology of CSVD, which is crucial for understanding its etiology, development, and clinical interventions. Investigating the differences and interconnections among these markers in follow-up studies is vital, as they hold practical significance in determining treatment plans and designing future studies. Linking these markers to clinical and pathophysiological mechanisms can significantly reduce the scale, duration, and cost of clinical trials (6).

CSVD has a diverse etiology, with arteriosclerosis and accumulation of amyloid being the most commonly observed causes (3,7,8). Recent evidence has suggested an association between neurodegeneration and CSVD (3). The majority of patients attending memory clinics display varying degrees of brain alterations associated with both Alzheimer's disease (AD) and CSVD (9). Therefore, there is a need for biomarkers that capture both AD and CSVD, enabling the assessment of the extent and contribution of each disease within individual patients (9-11). Future studies should investigate the impact of CSVD progression on gray matter (GM) and white matter atrophy, ideally in combination with traditional markers of neurodegenerative diseases (12). Amide proton transfer (APT) imaging is an MRI technique that reflects the protein and polypeptide content in tissues (10,13). The concentration of mobile proteins and semi-solid macromolecular proteins in the brain tissue increases with the severity of lesion in the neurodegenerative disease population, with the deposition of abnormal protein in the hippocampus being the most prominent. A previous study verified that the novel APT imaging could be an imaging marker for detecting abnormal protein deposition and vascular cognitive impairment in the hippocampus of patients with CSVD (14).

Linking APT imaging to CSVD raises 2 crucial questions. The first pertains to whether distinct CSVD image markers exhibit varied associations with APT values; the second delves into the capability of APT to reflect the severity of CSVD. Based on these considerations, we hypothesized that the association between different CSVD imaging markers and the extent of neurodegeneration could be indirectly confirmed by assessing the relationship between CSVD imaging markers and the hippocampal APT values. To our knowledge, this is the first study to indirectly investigate the mechanistic question of neurodegeneration in CSVD using *in vivo* imaging methods. The aim of this study was to explore potential differences in hippocampal APT values between CSVD imaging markers presence and absence groups and between groups with different CSVD total burden. The correlations between APT values and CSVD imaging markers were analyzed. The mediating effect of the hippocampal APT values in the association between CSVD total loads and Montreal Cognitive Assessment (MoCA) score was also assessed. We present this article in accordance with the STROBE reporting checklist (available

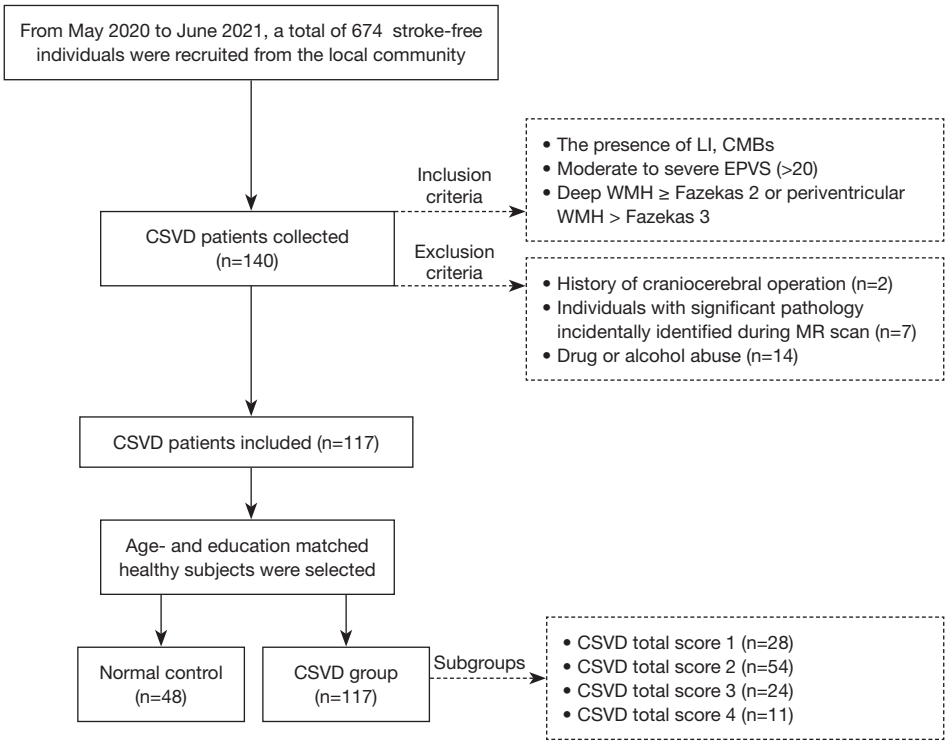

Figure 1 Flowchart shows inclusion and exclusion process of the present study. CSVD, cerebral small vessel disease; LI, lacunar infarction; CMB, cerebral microbleeding; EPVS, enlarged perivascular space; WMH, white matter hyperintensity; MR, magnetic resonance.

at https://qims.amegroups.com/article/view/10.21037/qims-23-1464/rc).

Methods

Participants

This study is part of an ongoing investigation of CSVD using multi-parametric MRI (retrospective analysis of prospectively-acquired data). A community-based cross-sectional study was conducted at Nanxishan Hospital of Guangxi Zhuang Autonomous Region. From May 2020 to June 2021, a total of 674 stroke-free individuals were recruited from the local community. The inclusion criteria for the participants were as follows: (I) the presence of LI, CMBs; (II) moderate-to-severe EPVS (>20); (III) deep WMH > Fazekas 2 or periventricular WMH > Fazekas 3. The exclusion criteria comprised the following: (I) history of craniocerebral operation; (II) cases with significant pathology incidentally identified during MR scan; (III) drug or alcohol abuse. A total of 48 age- and education-matched healthy individuals were selected from the local community as normal controls. *Figure 1* shows the process of inclusion and exclusion in this study. The study was conducted in accordance with the Declaration of Helsinki (as revised in 2013). This study sought approval from the Ethics Committee of Nanxishan Hospital of Guangxi Zhuang Autonomous Region (2020NXSYEC-006). Informed consent forms were signed by all participants. All demographic characteristics of the participants [including gender, age, body mass index (BMI), and education] were collected. A skilled neuro-radiologist (R.M. with 5 years of experience of neuro-radiology) conducted the cognitive assessment of each participant using the Beijing version of the MoCA. This information was gathered within 1 week preceding the MRI examination.

MRI data acquisition

In this study, MRI scans were performed using a 3.0-T MR system (Ingenia 3.0CX; Philips Healthcare, Best, The Netherlands) and 32-channel head coils. The specific scan sequences utilized in this study were as follows: A 3D T1-weighted fast field echo with a repetition time (TR) of 6.4 ms and an echo time (TE) of 3.0 ms, field of vision (FOV)

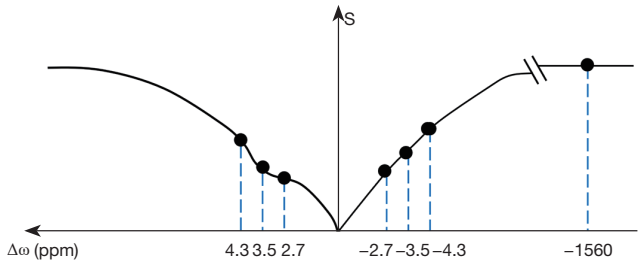

Figure 2 Diagram of the APT imaging acquisition. APT images were obtained using nine frequency offsets (4.3 ppm, repeated 3 times at 3.5, 2.7, –2.7, –3.5, –4.3, –1,560 ppm) relative to the water frequency. For the 3.5 ppm acquisition, a Dixon-based method was employed, and the acquisition window was shifted by ±0.4 and 0 ms, respectively. APT, amide proton transfer.

of 240 mm × 240 mm × 180 mm, reconstruction voxel of 1.1×1.1×1.1 mm^3, and a reconstruction matrix of 400×400, with a slice thickness of 1.1 mm. The utilization of T2 fast spin echo was implemented with a TR of 2,500 ms and a TE of 232 ms. The FOV was set at 250 mm × 25 mm × 180 mm, the reconstruction voxel at 1.1×1.1×1.1 mm^3, and the reconstruction matrix at 512×512, with a slice thickness of 1.1 mm. 3D fluid-attenuated inversion recovery (FLAIR) was conducted with a TR of 4,800 ms and a TE of 244 ms. A FOV of 240 mm × 240 mm × 173 mm, a reconstruction voxel size of 1.1×1.1×1.1 mm^3, and a reconstruction matrix of 384×384 were used, with a slice thickness of 1.2 mm. A 3D APT weight sequence was performed with a TR of 6,300 ms and a TE of 8.3 ms. The FOV was set at 230 mm × 180 mm × 60 mm, and the reconstruction voxel size was 1.8×1.8×6 mm^3, with a reconstruction matrix of 256×256 and a slice thickness of 6 mm. A turbo spin echo (TSE) factor of 174 was utilized. Prior to the routine sequences and APT sequence examination, each case underwent two shimming protocols. A 2-second APT pre-pulse with a saturation power level of B1, rms =2 mT was achieved for APT imaging by transmitting dual radiofrequency channels in an interleaved manner. APT images were obtained using 9 frequency offsets (4.3 ppm, repeated three times at 3.5, 2.7, –2.7, –3.5, –4.3, and –1,560 ppm) relative to the water frequency. For the 3.5 ppm acquisition, a Dixon-based method was employed, and the acquisition window was shifted by ±0.4 and 0 ms, respectively (*Figure 2*).

Image processing

Image processing was performed using the "IntelliSpace Portal" version 8 (Philips Healthcare) on an independent workstation. A radiologist, following the definitions established in a previous study (3), identified LI, WMH, CMB, and enlarged EPVS. The CSVD total burden was assessed using an ordinal scale from 1 to 4, with each of the following criteria assigned one point: the presence of LI, CMBs, moderate to severe EPVS (>20), and deep WMH ≥ Fazekas 2 or periventricular WMH > Fazekas 3 (7).

APT image data were reconstructed using the embedded program. The inhomogeneity effect of b0 fields was corrected as described in previous literature (15). The z-spectrum was fitted through all offsets on a voxel-by-voxel basis. The fitted curve was interpolated using an offset resolution of 1 Hz. After this step, the corresponding B0 field inhomogeneity was calculated according to the deviation of the minimum of the fitted curve from 0 ppm. To correct the field inhomogeneity effect, the original z-spectrum was interpolated and centered along the direction of the offset axis to shift its lowest intensity to 0 ppm. Finally, the APT-weighted image [namely, MTRasym (3.5 ppm) image] was calculated using the B0-corrected data at the offset of ±3.5 ppm.

The APT (%) calculation method was as follows (14):

$$\mathrm{MTRasym}\left([\Delta\omega]\right)=\frac{S(-\Delta\omega)-S(+\Delta\omega)}{S0}*100\% \quad [1]$$

When $\Delta\omega=+3.5$ ppm, one has: $\mathrm{APT}=\mathrm{MTRasym}\left(3.5\ \mathrm{ppm}\right)$

$$\mathrm{MTRasym}\left(3.5\ \mathrm{ppm}\right)=\frac{S(-3.5\ \mathrm{ppm})-S(+3.5\ \mathrm{ppm})}{S0}*100\% \quad [2]$$

Magnetic resonance ratio asymmetry (MTRasym) (3.5 ppm) is the abbreviation of magnetization transfer (MT) ratio asymmetry at 3.5 ppm. S0 represents the signal intensities without saturation pulse.

The APT images were co-registered and overlaid with the acquired FLAIR images, in cases where the sequences were not geometrically identical, coregistration was employed to ensure accurate alignment. Bilateral round or oval region of interest (ROI) measurements were conducted by two experienced radiologists, with 5 and 25 years of experience in neurological imaging, respectively. These measurements were taken to determine the APT intensity values in hippocampus. The size and shape of the ROI were determined based on the corresponding anatomical region. The normal APT intensity value was measured from the respective APT image. Mean APT intensity values of bilateral hippocampus were obtained separately, and the corresponding mean values of bilateral hippocampus were calculated.

Table 1 The difference of demographic characteristics and hippocampus APT values between the groups of CSVD total burden

Variables	CSVD total burden					*F*	P value
	0.0 (n=48)	1.0 (n=28)	2.0 (n=54)	3.0 (n=24)	4.0 (n=11)		
Age, years	57.40±8.51	55.04±5.93	55.78±8.46	56.38±7.72	57.82±9.50	0.546	0.702
Education, years	11.90±4.27	10.64±3.87	10.33±4.87	11.21±3.93	8.64±6.52	1.516	0.200
BMI, kg/m^2	24.67±2.70	24.94±3.50	24.73±2.87	23.12±2.62	24.78±1.70	1.723	0.147
Hippocampal APT, %	0.78±0.52[a]	0.81±0.27[a]	1.11±0.34[b]	1.26±0.30[b]	1.28±0.18[b]	11.180	<0.001

Data are presented as mean ± standard deviation. CSVD patients were divided into four subgroups. The difference in hippocampal APT values among different CSVD total load groups was found to be significant at the 0.01 level (F=11.180, P<0.001). Post-hoc comparisons showed no statistical difference in hippocampus APT values between groups 0 and 1, as well as between groups 2, 3, and 4. [a] and [b], no difference between the same letters. APT, amide proton transfer; CSVD, cerebral small vessel disease; BMI, body mass index.

Statistics analyses

Statistical analyses were performed using SPSS 26.0 (IBM Corp., Armonk, NY, USA). A bilateral P value of less than 0.05 was considered statistically significant. The intra-class correlation coefficient (ICC) test was used to test the consistency of the ROI measurements of both radiologists, with an ICC score >0.7 indicating satisfactory agreement between them. Means of the variables measured by 2 radiologists were used for statistical analysis. The Shapiro-Wilk test was used to test for normality and homogeneity of variance.

Gender data were presented in cases, and the chi-square test was used to test for differences between groups. Normally distributed data were presented as mean ± standard deviation. Demographic and APT variables between groups were compared using an independent *t*-test and one-way analysis of variance (ANOVA); the Bonferroni correction was used for post-hoc tests. Pearson correlation analysis was used to study correlations between APT values and CSVD imaging markers. According to Cohen's criteria (16), correlation coefficients (r) of 0.1≤r<0.3 indicated weak association, 0.3≤r<0.5 indicated moderate association, and r≥0.5 indicated strong association.

A mediation analysis model was used to investigate the mediating effect of the mean hippocampus APT value in the association between CSVD total loads and MoCA score. The mediation analysis is based on the estimation of the four pathways. The a path represents the regression analysis of CSVD total load and the APT value of the hippocampus. The b path represents the regression analysis of the APT value of the hippocampus and MoCA score. The c path represents the regression analysis of CSVD total load and MoCA score. The c' path represents the c path regression analysis model including the mediation variable (the APT value of the hippocampus). The proportion of mediation attributable to the models was calculated as (a*b/c).

Results

Demographic and clinical characteristics of the participants

A total of 117 cases were included in the final analysis. According to the CSVD total score, CSVD patients were divided into 4 subgroups, including 28 cases in group of CSVD =1, 54 cases in group of CSVD =2, 24 cases in group of CSVD =3, and 11 cases in group of CSVD =4. A further 48 age- and education-matched healthy individuals were selected as normal controls, recording as CSVD =0. Detailed demographic and clinical data are presented in *Table 1*. There were no significant differences in age, education, and BMI in the CSVD total burden groups. Out of the 117 patients with CSVD, there were 27 cases of LI, 64 cases of WMH, 55 cases of EPVS, and 24 cases of CMB (*Table 2*).

Reliability of measurements

The measurements taken by both observers were highly consistent (P>0.05). The ICC was found to be 0.806 and 0.814 for bilateral hippocampal APT values, respectively.

The comparison of demographic characteristics and hippocampus APT values between the groups of CSVD total burden

The difference in hippocampal APT values among different CSVD total load groups was found to be significant at the

Table 2 The deference of hippocampus APT value between the groups of CSVD imaging markers presence or not

Imaging markers	N (%)	Hippocampus APT, mean ± SD		*t* value	P value
		Absence	Presence		
LI	27 (23.08)	0.92±0.39	1.30±0.43	–4.764	<0.001**
WMH	64 (54.70)	0.82±0.42	1.14±0.37	–5.204	<0.001**
EPVS	55 (47.01)	0.94±0.43	1.08±0.41	–2.143	0.034*
CMB	24 (20.51)	0.95±0.43	1.23±0.30	–3.105	0.002**

The comparison results indicated that the APT value of the hippocampus was higher in the groups with imaging markers compared to the imaging marker absence groups. *, P<0.05; **, P<0.01. APT, amide proton transfer; CSVD, cerebral small vessel disease; SD, standard deviation; LI, lacunar infarction; WMH, white matter hyperintensity; EPVS, enlarged perivascular space; CMB, cerebral microbleeding.

Table 3 The correlation of hippocampus APT value with CSVD imaging markers

Variables	r	P value
LI	0.346	<0.01
WMH	0.375	<0.01
EPVS	0.136	0.082
CMB	0.290	<0.01

Pearson correlation analyses revealed a weak to moderate but significant correlation between the APT values and the CSVD imaging markers except EPVS. APT, amide proton transfer; CSVD, cerebral small vessel disease; SD, standard deviation; LI, lacunar infarction; WMH, white matter hyperintensity; EPVS, enlarged perivascular space; CMB, cerebral microbleeding.

0.01 level (F=11.180, P<0.001). This suggested that there was a difference of APT values in hippocampus between groups. The mean hippocampal APT values of the different CSVD total loads were ranked as follows: 4>3>2>1>0. Post-hoc comparisons showed no statistical difference in hippocampus APT values between groups 0 and 1, as well as between groups 2, 3, and 4 (*Table 1*).

The comparison of hippocampus APT values between the groups of CSVD imaging marker presence and absence groups

The APT values of the hippocampus were significantly different between the groups with CSVD imaging marker presence and absence groups. The P values for the LI, WMH, EPVS, and CMB presence and absence groups were <0.001, <0.001, 0.034, and 0.002, respectively. The comparison results indicated that the APT value of the hippocampus was higher in the groups with imaging markers compared to the imaging marker absence groups (*Table 2*).

Correlation analysis of hippocampus APT values with CSVD imaging markers

Pearson correlation analyses revealed a weak but significant correlation between the APT value of the hippocampus and CMB (r=0.290, P<0.01). Furthermore, the APT value of the hippocampus displayed moderate but significant correlations with LI (r=0.346, P<0.01) and WMH (r=0.375, P<0.01). However, the APT value of the hippocampus did not show a significant correlation with EPVS, as indicated by Pearson correlation analyses (*Table 3*).

Mediation effect of hippocampal APT on cognitive impairment caused by CSVD total load

The regression coefficient (c) in the regression analysis of CSVD total load and MoCA score was –3.551 [95% confidence interval (CI): –4.033 to –3.070, P<0.001]. After including the mediation variable in the regression analysis model, the regression coefficient (c') of CSVD total load and MoCA score was –2.932 (95% CI: –3.429 to –2.435, P<0.001). The regression coefficient (a) for the regression analysis of CSVD total load and the APT value of the hippocampus was 0.154 (95% CI: 0.107 to 0.201, P<0.001). Furthermore, the regression coefficient (b) for the regression analysis of the APT value of the hippocampus and MoCA score was –4.033 (95% CI: –5.484 to –2.582, P<0.001).

The mediation models demonstrated that the APT value of the hippocampus partially mediated the association between CSVD total load and MoCA score, as evidenced in *Table 4*. The proportion of mediation attributable to the

Table 4 Mediation effect of hippocampal APT on cognitive impairment caused by CSVD total load

Mediation analysis	Mediation symbol	Regression coefficient	95% CI		z/*t* value	P value
			Lower limit	Upper limit		
CSVD→Hip APT→MoCA	a*b	−0.619	−0.236	−0.064	−13.987	<0.001
CSVD→Hip APT	a	0.154	0.107	0.201	6.407	<0.001
Hip APT→MoCA	b	−4.033	−5.484	−2.582	−5.446	<0.001
CSVD→MoCA	c’	−2.932	−3.429	−2.435	−11.563	<0.001
CSVD→MoCA	c	−3.551	−4.033	−3.070	−14.451	<0.001

The mediation models demonstrated that the APT value of the hippocampus partially mediated the association between CSVD total load and MoCA score. APT, amide proton transfer; CSVD, cerebral small vessel disease; CI, confidence interval; Hip, hippocampus; MoCA, Montreal Cognitive Scale.

models was calculated as 17.50% (a*b/c) (*Table 4*).

Discussion

In the present study, we investigated the relationship between hippocampal APT values, CSVD imaging markers, and CSVD total load. The findings were as follows: (I) the APT value of the hippocampus was higher in the presence of imaging markers compared to the control groups; (II) there was a gradual increase in APT values of the hippocampus with an increase in the total CSVD load; (III) the APT value of the hippocampus showed a significant correlation with the CSVD imaging markers; (IV) the APT value of the hippocampus partially mediated the association between CSVD total load and MoCA score.

APT is a protein content-dependent chemical exchange saturation transfer (CEST) MRI technique (17). The chemical exchange rate has been shown to be primarily related to the concentration of amide protons (66%) and the pH value (33%) in the tissue. Additionally, temperature can also have a partial effect on the chemical exchange rate (18). Due to the lack of significant differences in temperature or pH values between the brains of CSVD patients and the normal elderly population, the APT values almost entirely reflect the variations in amide proton concentration (14). Mild cognitive impairment (MCI) and AD are associated with the accumulation of abnormal proteins in the brain. Previous studies have verified that the deposition of abnormal proteins in the hippocampus in patients with MCI and AD results in APT values being significantly higher than those in normal elderly people of the same age (14,15). This indicates that APT is a potential method that can non-invasively visualize the protein content *in vivo*.

The hippocampus is known to be susceptible to aging and neurodegeneration (19-21). The first result of this study showed a higher hippocampal APT value in the imaging markers presence groups compared to the imaging markers absence groups. These findings suggest a potential association between the presence of CSVD imaging markers and neurodegeneration. It is well-known that neurodegenerative diseases often coexist with CSVD. Patients with CSVD face an increased risk of developing Parkinson’s disease (PD) when combined with WMH lesions or multiple LIs, particularly in the frontal lobe (12). Bergkamp *et al.* reported that individuals who developed PD exhibited a higher baseline CSVD load (12). The association between the presence of baseline LIs and the onset of PD was predominantly driven by LIs located in the frontal lobe and basal ganglia. Meanwhile, WMHs in all lobes were associated with the onset of PD (12). Soldan *et al.* revealed that a higher baseline WMH load promotes the progression of AD pathology. Additionally, the authors found a significant correlation between baseline WMH volume and time to AD symptom onset (22). Fan *et al.* also reported a significant association between WMH and medial temporal atrophy (23). Although previous studies have demonstrated the synergistic interactions between medial temporal atrophy and CSVD, these studies primarily focused on separate CSVD features such as WMH and LIs (24-26). Van der Flier *et al.* discovered an additive effect of WMH and medial temporal atrophy, providing further evidence for the combined involvement of both Alzheimer’s-type pathology and vascular pathology in the initial stages of cognitive decline (24). Wong *et al.* demonstrated that medial temporal atrophy is associated with a higher burden of CSVD among patients with

amnestic-type dementia, suggesting that CSVD might be an important mechanism behind hippocampal atrophy (25). These findings have implications for clinical management strategies, where interventions to reduce cerebrovascular disease may potentially slow down neurodegeneration and disease progression (25). Jokinen *et al.* proposed that medial temporal, subcortical, and cortical atrophy may potentiate the effect of WMH and LIs on cognitive decline (27). The relationship between CSVD imaging markers and neurodegeneration is likely a bidirectional pathophysiological process. Firstly, neurodegeneration may accelerate the development of certain CSVD imaging markers. For example, elevated b-secretase levels, as a key enzyme in amyloidogenesis of amyloid precursor proteins, can result in white matter contraction and damage, thereby disrupting the connection of projection fibers in this area (28,29). Tau protein, playing a crucial role in AD pathology, ultimately disrupts neuronal microstructure through the formation of neurofibrillary tangles, leading to gray and white matter damage and secondary brain atrophy (30,31). Secondly, a higher CSVD total load may further accelerate the occurrence of secondary neurodegenerative diseases (32). Previous research has suggested that LIs are associated with WMH features, and both of these correspond to secondary neurodegeneration, increased mortality, and poor functional prognosis (30). Aribisala *et al.* asserted that asymptomatic LIs are associated with brain atrophy, disruption of white matter integrity, and subsequent cognitive decline, suggesting their potential role in neurodegenerative diseases (5). Discrete subcortical infarcts induce the loss of connected cortex far from the infarct through white matter tract degeneration (26). Increasing WMH burden is associated with worse whole-brain atrophy and thinning of the cortex overlying areas with higher WMH density (33). In addition, neurodegeneration and CSVD may have interconnected and mutually reinforcing pathophysiological processes. The clinical differentiation between AD and CSVD becomes blurred due to shared risk factors and mechanisms of occurrence (3,34-36). CSVD imaging markers, such as LIs and CMBs, may appear at various time points during disease progression or may be absent. As the disease advances, concurrent CSVD imaging markers increase, indicating a higher total CSVD load and more complex, severe pathophysiological processes. A higher CSVD load may also accompany more severe neurodegeneration, which was supported by an additional finding in this study. We observed a gradual increase in hippocampal APT values with an increasing total CSVD load. CSVD imaging markers and secondary cortical thinning impose a greater burden on long tract degeneration, exacerbating neurodegeneration (32). An increased CSVD total load induces secondary gray and white matter loss in affected brain regions, resulting in brain atrophy and neurodegeneration.

An additional finding of this study is that the mediation models revealed the partial mediating effect of the hippocampal APT value on the relationship between the CSVD total load and the MoCA score. It is worth noting that mixed neurodegeneration and CSVD pathology are frequently observed in the same group of patients, and this pattern becomes more common with increasing age (10). However, it should be noted that only a small number of patients with CSVD actually develop parkinsonism, indicating that other factors contribute to this outcome (37). The mediation proportion accounted for 17.50% in this study, indicating that neurodegeneration can only partially explain the cognitive impairment caused by CSVD. It is possible that the impairment of neural signal conduction in different neural circuits due to damage of the invisible microstructure caused by vascular pathophysiological changes plays a significant role in the clinical symptoms of CSVD patients (38). From a clinical perspective, the exact interaction between CSVD and neurodegenerative diseases is still a subject of debate (39).

T1 relaxation time is another factor affecting APT MRI signals. Shortening the T1 relaxation time can reduce APT values and the detectability of mobile protein levels (40). CSVD primarily affects T2 relaxation time rather than T1 (41). Therefore, changes in T1 relaxation time in CSVD patients may have minimal impact on the APT signal. In addition, the ideal Z-spectrum can differentiate various exchangeable proton components, indirectly measuring the actual concentration of each substance. However, aside from the chemical exchange effect, the Z spectrum encompasses other influencing factors, including traditional MT effect, direct water saturation (DS), and nuclear Overhauser enhancement (NOE) (42). Additionally, endogenous metabolites exhibit closely distributed frequencies and differing content distribution, resulting in overlapping metabolite peaks. This complicates the accurate retrieval of concentration information from spectral lines. The asymmetric MT rate could be applied to remove the MT effect, but the extraction and analysis of CEST signals invariably introduce the NOE effect (43). Metabolites suitable for *in vivo* CEST imaging tend to have sites with the same frequency size on the opposite side of the

water peak, which largely corresponds to the NOE effect. This characteristic results in a relatively reduced signal attenuation caused by chemical shift. Nevertheless, the high APT-weighted signal consistently observed in patients with AD and the ability to differentiate AD from normal cases make the APT-weighted MRI signal a powerful clinical biomarker for CSVD detection.

In a clinical setting, the early detection of abnormal hippocampal APT values may serve as a sensitive biomarker for the onset of neurodegeneration in CSVD patients. Abnormal hippocampal APT values indicate the coupling between neurodegeneration and CSVD. However, further research is needed to comprehensively investigate the trajectory of neurodegeneration in CSVD patients, as distinguishing CSVD from neurodegenerative diseases remains challenging.

There were several limitations to this study. Firstly, it was a cross-sectional study conducted on a specific population within a local community. As a result, our conclusions cannot be generalized to the broader population, and the lack of follow-up hindered our ability to assess the longitudinal evolution of neurodegeneration in CSVD patients. Secondly, the sample size in this study was relatively small. This might not fully capture the true differences in hippocampal APT values between various imaging markers and CSVD total load groups. Conducting studies with larger sample sizes would be more likely to provide an accurate trajectory of CSVD neurodegeneration. Thirdly, the presence and accumulation of CSVD imaging markers may lead to limitations in the comparison between the imaging marker presence group and the control group. This comparison only reflects a trend when the marker is aggregated and cannot completely eliminate the effects of other CSVD imaging markers. Finally, this study solely focused on comparing differences in hippocampal APT values between different imaging markers. It did not consider the combination of cerebrospinal fluid or blood neurodegenerative markers. Thus, it does not provide a comprehensive reflection of neurodegeneration in the population.

Conclusions

This study demonstrated differences in hippocampus APT values between CSVD imaging markers and control groups and between groups with different CSVD total scores. APT values in the hippocampus were correlated with CSVD imaging markers. Hippocampal APT value may serve as a biomarker for the early detection of neurodegeneration in CSVD patients.

Acknowledgments

The authors express their gratitude to the dedicated staff of subject group of cerebral small vascular disease.

Funding: This work was supported by following funding programs: Social Development Program of Guilin Science and Technology Bureau (2020011206-7, 20210227-9-2); Health Development Program of Guangxi Zhuang Autonomous Region (Z20191023); The Excellence Project of Nanxishan Hospital in Guangxi Zhuang Autonomous Region (NY2019003); Natural Science Foundation of Guangxi Autonomous Region (2023GXNSFAA026383).

Footnote

Reporting Checklist: The authors have completed the STROBE reporting checklist. Available at https://qims.amegroups.com/article/view/10.21037/qims-23-1464/rc

Conflicts of Interest: All authors have completed the ICMJE uniform disclosure form (available at https://qims.amegroups.com/article/view/10.21037/qims-23-1464/coif). K.D. is employed by Philips (China) Investment Co., Ltd., Guangzhou Branch. The other authors have no conflicts of interest to declare.

Ethical Statement: The authors are accountable for all aspects of the work in ensuring that questions related to the accuracy or integrity of any part of the work are appropriately investigated and resolved. The study was conducted in accordance with the Declaration of Helsinki (as revised in 2013). The study was approved by the Ethics Committee of Nanxishan Hospital of Guangxi Zhuang Autonomous Region (2020NXSYEC-006) and informed consent was provided by all participants.

References

1. Wardlaw JM. William M. Feinberg Award for Excellence in Clinical Stroke: Small Vessel Disease; a Big Problem, But Fixable. Stroke 2018;49:1770-5.
2. Pantoni L. Cerebral small vessel disease: from pathogenesis and clinical characteristics to therapeutic challenges. Lancet Neurol 2010;9:689-701.
3. Wardlaw JM, Smith EE, Biessels GJ, Cordonnier C, Fazekas F, Frayne R, et al. Neuroimaging standards for research into small vessel disease and its contribution to ageing and neurodegeneration. Lancet Neurol 2013;12:822-38.
4. Pasi M, Cordonnier C. Clinical Relevance of Cerebral Small Vessel Diseases. Stroke 2020;51:47-53.
5. Aribisala BS, Valdés Hernández MC, Royle NA, Morris Z, Muñoz Maniega S, Bastin ME, Deary IJ, Wardlaw JM. Brain atrophy associations with white matter lesions in the ageing brain: the Lothian Birth Cohort 1936. Eur Radiol 2013;23:1084-92.
6. Benjamin P, Zeestraten E, Lambert C, Ster IC, Williams OA, Lawrence AJ, Patel B, MacKinnon AD, Barrick TR, Markus HS. Progression of MRI markers in cerebral small vessel disease: Sample size considerations for clinical trials. J Cereb Blood Flow Metab 2016;36:228-40.
7. Cannistraro RJ, Badi M, Eidelman BH, Dickson DW, Middlebrooks EH, Meschia JF. CNS small vessel disease: A clinical review. Neurology 2019;92:1146-56.
8. Cuadrado-Godia E, Dwivedi P, Sharma S, Ois Santiago A, Roquer Gonzalez J, Balcells M, Laird J, Turk M, Suri HS, Nicolaides A, Saba L, Khanna NN, Suri JS. Cerebral Small Vessel Disease: A Review Focusing on Pathophysiology, Biomarkers, and Machine Learning Strategies. J Stroke 2018;20:302-20.
9. Kapasi A, DeCarli C, Schneider JA. Impact of multiple pathologies on the threshold for clinically overt dementia. Acta Neuropathol 2017;134:171-86.
10. Attems J, Jellinger KA. The overlap between vascular disease and Alzheimer's disease--lessons from pathology. BMC Med 2014;12:206.
11. Beach TG, Malek-Ahmadi M. Alzheimer's Disease Neuropathological Comorbidities are Common in the Younger-Old. J Alzheimers Dis 2021;79:389-400.
12. Bergkamp MI, Tuladhar AM, van der Holst HM, van Leijsen EMC, Ghafoorian M, van Uden IWM, van Dijk EJ, Norris DG, Platel B, Esselink RAJ, Leeuw FE. Brain atrophy and strategic lesion location increases risk of parkinsonism in cerebral small vessel disease. Parkinsonism Relat Disord 2019;61:94-100.
13. Khan W, Egorova N, Khlif MS, Mito R, Dhollander T, Brodtmann A. Three-tissue compositional analysis reveals in-vivo microstructural heterogeneity of white matter hyperintensities following stroke. Neuroimage 2020;218:116869.
14. Guo Z, Jiang Y, Qin X, Mu R, Meng Z, Zhuang Z, Liu F, Zhu X. Amide Proton Transfer-Weighted MRI Might Help Distinguish Amnestic Mild Cognitive Impairment From a Normal Elderly Population. Front Neurol 2021;12:707030.
15. Wang R, Li SY, Chen M, Zhou JY, Peng DT, Zhang C, Dai YM. Amide proton transfer magnetic resonance imaging of Alzheimer's disease at 3.0 Tesla: a preliminary study. Chin Med J (Engl) 2015;128:615-9.
16. Faul F, Erdfelder E, Lang AG, Buchner A. G*Power 3: a flexible statistical power analysis program for the social, behavioral, and biomedical sciences. Behav Res Methods 2007;39:175-91.
17. Sun C, Zhao Y, Zu Z. Evaluation of the molecular origin of amide proton transfer-weighted imaging. Magn Reson Med 2024;91:716-34.
18. Zhou J, Heo HY, Knutsson L, van Zijl PCM, Jiang S. APT-weighted MRI: Techniques, current neuro applications, and challenging issues. J Magn Reson Imaging 2019;50:347-64.
19. Geinisman Y, Detoledo-Morrell L, Morrell F, Heller RE. Hippocampal markers of age-related memory dysfunction: behavioral, electrophysiological and morphological perspectives. Prog Neurobiol 1995;45:223-52.
20. Raz N, Lindenberger U, Rodrigue KM, Kennedy KM, Head D, Williamson A, Dahle C, Gerstorf D, Acker JD. Regional brain changes in aging healthy adults: general trends, individual differences and modifiers. Cereb Cortex 2005;15:1676-89.
21. Barnes J, Bartlett JW, van de Pol LA, Loy CT, Scahill RI, Frost C, Thompson P, Fox NC. A meta-analysis of hippocampal atrophy rates in Alzheimer's disease. Neurobiol Aging 2009;30:1711-23.
22. Soldan A, Pettigrew C, Zhu Y, Wang MC, Moghekar A, Gottesman RF, Singh B, Martinez O, Fletcher E, DeCarli C, Albert M; . White matter hyperintensities and CSF Alzheimer disease biomarkers in preclinical Alzheimer disease. Neurology 2020;94:e950-60.
23. Fan Y, Shen M, Huo Y, Gao X, Li C, Zheng R, Zhang J. Total Cerebral Small Vessel Disease Burden on MRI Correlates With Medial Temporal Lobe Atrophy and Cognitive Performance in Patients of a Memory Clinic.

Front Aging Neurosci 2021;13:698035.
24. van der Flier WM, van Straaten EC, Barkhof F, Ferro JM, Pantoni L, Basile AM, Inzitari D, Erkinjuntti T, Wahlund LO, Rostrup E, Schmidt R, Fazekas F, Scheltens P; . Medial temporal lobe atrophy and white matter hyperintensities are associated with mild cognitive deficits in non-disabled elderly people: the LADIS study. J Neurol Neurosurg Psychiatry 2005;76:1497-500.
25. Wong BYX, Yong TT, Lim L, Tan JY, Ng ASL, Ting SKS, Hameed S, Ng KP, Zhou JH, Kandiah N. Medial Temporal Atrophy in Amyloid-Negative Amnestic Type Dementia Is Associated with High Cerebral White Matter Hyperintensity. J Alzheimers Dis 2019;70:99-106.
26. Ghaznawi R, Geerlings MI, Jaarsma-Coes MG, Zwartbol MH, Kuijf HJ, van der Graaf Y, Witkamp TD, Hendrikse J, de Bresser J. The association between lacunes and white matter hyperintensity features on MRI: The SMART-MR study. J Cereb Blood Flow Metab 2019;39:2486-96.
27. Jokinen H, Lipsanen J, Schmidt R, Fazekas F, Gouw AA, van der Flier WM, Barkhof F, Madureira S, Verdelho A, Ferro JM, Wallin A, Pantoni L, Inzitari D, Erkinjuntti T; . Brain atrophy accelerates cognitive decline in cerebral small vessel disease: the LADIS study. Neurology 2012;78:1785-92.
28. Fukumoto H, Cheung BS, Hyman BT, Irizarry MC. Beta-secretase protein and activity are increased in the neocortex in Alzheimer disease. Arch Neurol 2002;59:1381-9.
29. Chalmers K, Wilcock G, Love S. Contributors to white matter damage in the frontal lobe in Alzheimer's disease. Neuropathol Appl Neurobiol 2005;31:623-31.
30. Sanford AM. Mild Cognitive Impairment. Clin Geriatr Med 2017;33:325-37.
31. Cummings JL, Cole G. Alzheimer disease. JAMA 2002;287:2335-8.
32. Wardlaw JM, Smith C, Dichgans M. Small vessel disease: mechanisms and clinical implications. Lancet Neurol 2019;18:684-96.
33. Lambert C, Benjamin P, Zeestraten E, Lawrence AJ, Barrick TR, Markus HS. Longitudinal patterns of leukoaraiosis and brain atrophy in symptomatic small vessel disease. Brain 2016;139:1136-51.
34. Schneider JA, Arvanitakis Z, Bang W, Bennett DA. Mixed brain pathologies account for most dementia cases in community-dwelling older persons. Neurology 2007;69:2197-204.
35. Dichgans M, Zietemann V. Prevention of vascular cognitive impairment. Stroke 2012;43:3137-46.
36. Brayne C, Richardson K, Matthews FE, Fleming J, Hunter S, Xuereb JH, Paykel E, Mukaetova-Ladinska EB, Huppert FA, O'Sullivan A, Dening T; . Neuropathological correlates of dementia in over-80-year-old brain donors from the population-based Cambridge city over-75s cohort (CC75C) study. J Alzheimers Dis 2009;18:645-58.
37. van der Holst HM, van Uden IW, Tuladhar AM, de Laat KF, van Norden AG, Norris DG, van Dijk EJ, Esselink RA, Platel B, de Leeuw FE. Cerebral small vessel disease and incident parkinsonism: The RUN DMC study. Neurology 2015;85:1569-77.
38. Hirsiger S, Koppelmans V, Mérillat S, Erdin C, Narkhede A, Brickman AM, Jäncke L. Executive Functions in Healthy Older Adults Are Differentially Related to Macro- and Microstructural White Matter Characteristics of the Cerebral Lobes. Front Aging Neurosci 2017;9:373.
39. Kahl A, Blanco I, Jackman K, Baskar J, Milaganur Mohan H, Rodney-Sandy R, Zhang S, Iadecola C, Hochrainer K. Cerebral ischemia induces the aggregation of proteins linked to neurodegenerative diseases. Sci Rep 2018;8:2701.
40. Qin X, Mu R, Zheng W, Li X, Liu F, Zhuang Z, Yang P, Zhu X. Comparison and combination of amide proton transfer magnetic resonance imaging and the apparent diffusion coefficient in differentiating the grades of prostate cancer. Quant Imaging Med Surg 2023;13:812-24.
41. Brandhofe A, Stratmann C, Schüre JR, Pilatus U, Hattingen E, Deichmann R, Nöth U, Wagner M, Gracien RM, Seiler A. T(2) relaxation time of the normal-appearing white matter is related to the cognitive status in cerebral small vessel disease. J Cereb Blood Flow Metab 2021;41:1767-77.
42. van Zijl PCM, Lam WW, Xu J, Knutsson L, Stanisz GJ. Magnetization Transfer Contrast and Chemical Exchange Saturation Transfer MRI. Features and analysis of the field-dependent saturation spectrum. Neuroimage 2018;168:222-41.
43. Hua J, Jones CK, Blakeley J, Smith SA, van Zijl PC, Zhou J. Quantitative description of the asymmetry in magnetization transfer effects around the water resonance in the human brain. Magn Reson Med 2007;58:786-93.

Cite this article as: Mu R, Qin X, Zheng W, Yang P, Huang B, Li X, Liu F, Deng K, Zhu X. Hippocampal amide proton transfer values are associated with cerebral small vessel disease imaging markers and total burden: a community-based cross-sectional study. Quant Imaging Med Surg 2024;14(3):2603-2613. doi: 10.21037/qims-23-1464

